

Helical Structures
How to cite: *Angew. Chem. Int. Ed.* **2023**, *62*, e202212571

International Edition: doi.org/10.1002/anie.202212571

German Edition: doi.org/10.1002/ange.202212571

Light-Controlled Destruction and Assembly: Switching between Two Differently Composed Cage-Type Complexes

Daniel Hugenbusch, Marc Lehr, Jan-Simon von Glasenapp, Anna J. McConnell,* and Rainer Herges*

Abstract: We report on two regioisomeric, diazocine ligands **1** and **2** that can both be photoswitched between the *E*- and *Z*-configurations with violet and green light. The self-assembly of the four species (**1-Z**, **1-E**, **2-Z**, **2-E**) with Co^{II} ions was investigated upon changing the coordination vectors as a function of the ligand configuration (*E* vs *Z*) and regioisomer (**1** vs **2**). With **1-Z**, Co₂(**1-Z**)₃ was self-assembled, while a mixture of ill-defined species (oligomers) was observed with **2-Z**. Upon photoswitching with 385 nm to the *E* configurations, the opposite was observed with **1-E** forming oligomers and **2-E** forming Co₂(**2-E**)₃. Light-controlled dis/assembly was demonstrated in a ligand competition experiment with sub-stoichiometric amounts of Co^{II} ions; alternating irradiation with violet and green light resulted in the reversible transformation between Co₂(**1-Z**)₃ and Co₂(**2-E**)₃ over multiple cycles without significant fatigue by photoswitching.

Triggered and controlled assembly and disassembly are among the most fundamental processes in living systems. For instance, light-triggered *cis* to *trans* isomerisation of retinal inside rhodopsin ultimately leads to the macroscopic perception of light following several consecutive processes, including the assembly of two rhodopsins with transducin and disassembly of the heterotrimeric transducin into two of its three components.^[1] Stimulus-controlled assembly and disassembly are ubiquitous steps in biological signal transduction cascades. In natural and synthetic systems, light is an almost ideal stimulus and control tool since it can be applied with high spatiotemporal resolution with different wavelengths, and it is typically waste- and by-product-free.^[2] Light has been exploited to trigger the self-assembly of nanoparticles,^[3] polymers^[4] and gels^[4a,5] as well as to drive

the folding of polymers^[6] and the operation of molecular machines^[7] and shuttles.^[8]

Despite the numerous examples of stimuli-responsive metal-organic cages and helicates,^[2,9] light-responsive examples are relatively rare and include the use of photoswitchable guests and counterions^[10] as well as photo-induced metal-ligand bond breakage,^[11] photolabile groups^[12] or photoacids^[13] to trigger the self-assembly/disassembly of cages. Photoswitchable cages^[2] based on azobenzene,^[14] dithienylethene,^[15] overcrowded alkenes,^[16] and more recently, diazocine^[17] have been reported but are challenging to design; for example, incomplete photoswitching (from overlapping n-π* and π-π* bands or overlap with the metal's MLCT band) can lead to isomeric mixtures and large ligand geometry changes upon photoswitching can produce ill-defined self-assemblies.^[2,9a,14b] Beves et al. recently reported on a photoswitchable, azobenzene-based Pd complex that switches between two different complex geometries and stoichiometries upon irradiation with two different wavelengths of visible light.^[14c]

Recently, diazocines (bridged azobenzenes) were developed as a new type of photoswitch with promising properties for applications, ranging from photopharmacology^[18] to switchable surfaces^[19] and smart materials.^[20] The good separation of n-π* and π-π* bands, efficient photoswitching with visible light and the thermodynamic stability of the *Z* configuration (as opposed to the *E* configuration for azobenzenes) make diazocines appealing for the design of photoswitchable cages. However, the development of diazocine-based, photoswitchable cages is in its infancy. Clever et al. recently reported on a photoresponsive, diazocine-based Pd₂L₄ cage.^[17] Upon irradiation with two different wavelengths, the complex reversibly changes its cage volume and binds or releases a guest.

We report that violet and green light direct the outcome of self-assembly in a competition experiment with Co^{II} ions and a mixture of the two photoswitchable regioisomeric diazocine ligands, **1** and **2** (Figure 1). In their thermodynamically stable *Z* form, Co₂(**1-Z**)₃ is self-assembled since **2-Z** does not form discrete self-assemblies with Co^{II} ions. Upon irradiation with violet light (385 nm) ligands **1** and **2** simultaneously switch to their metastable *E* form and metastable Co₂(**2-E**)₃ is self-assembled since ligand **1-E** forms ill-defined complexes with Co^{II}. Irradiation with green light (520 nm) switches both ligands simultaneously back to their original *Z* configuration, restoring the initial Co₂(**1-Z**)₃. Thus, we report the reversible photoswitching between Co₂(**1-Z**)₃ and Co₂(**2-E**)₃ without fatigue over a number of

[*] D. Hugenbusch, M. Lehr, J.-S. von Glasenapp, Prof. Dr. A. J. McConnell, Prof. Dr. R. Herges
 Otto-Diels-Institute of Organic Chemistry,
 Christian-Albrechts-Universität zu Kiel
 Otto-Hahn-Platz 4, 24118 Kiel (Germany)
 E-mail: amconnell@oc.uni-kiel.de
 rherges@oc.uni-kiel.de

© 2022 The Authors. Angewandte Chemie International Edition published by Wiley-VCH GmbH. This is an open access article under the terms of the Creative Commons Attribution License, which permits use, distribution and reproduction in any medium, provided the original work is properly cited.

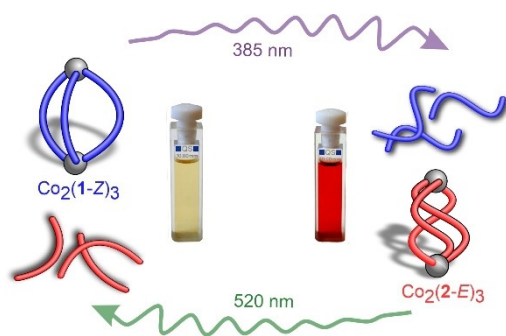


Figure 1. Reversible light-controlled assembly and disassembly of $\text{Co}_2(\mathbf{1-Z})_3$ and $\text{Co}_2(\mathbf{2-E})_3$. Self-assembly is directed with violet and green light. Ligands **1** and **2** are represented as blue and red “sausages”. Co^{2+} ions are grey spheres. *Z* isomers (*cis* azo group) have a C shape and *E* isomers (*trans*) an S shape. For an assignment to the corresponding chemical structures and DFT optimized geometries, see Figure 2. For the 2D chemical structures of **1** and **2** see Figure 3.

cycles. To the best of our knowledge, it is the first example of a reversible light-controlled transformation between two distinct metallosupramolecular structures including different ligands via dis/assembly.

Ligands **1** and **2** each consist of a diazocine-backbone and two 2-pyridyl-triazole units attached to both benzene rings (Figure 2). They differ in the point of attachment of the two pyridyl-triazole groups (*para* with respect to the azo group in **1** and *meta* in **2**), which gives rise to different

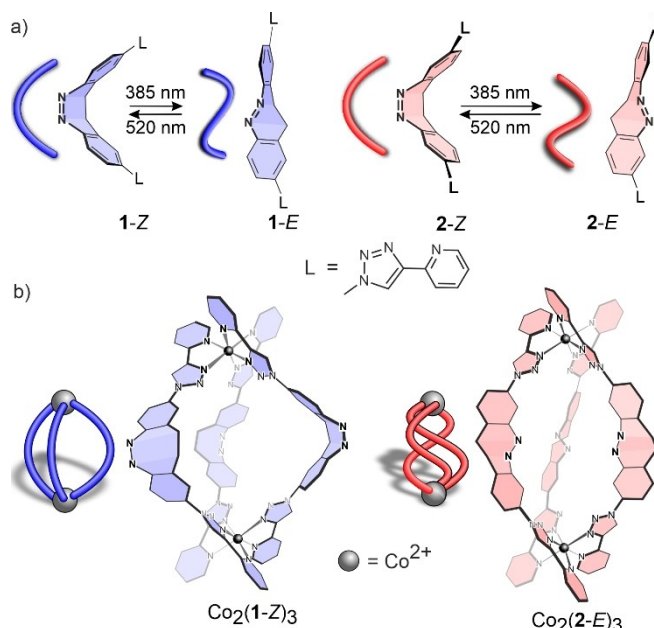


Figure 2. a) Photoswitchable diazocine-based, regioisomeric ligands **1** and **2** in their *Z* and *E* configurations. b) $\text{Co}_2(\mathbf{1-Z})_3$ and $\text{Co}_2(\mathbf{2-E})_3$ are the only defined self-assemblies formed from the four possible ligands (**1-Z**, **1-E**, **2-Z**, **2-E**) and Co^{II} ions. Ligands **1-E** and **2-Z** formed ill-defined complexes with Co^{II} ions. Note in (b) double bonds are omitted for clarity and the ligand “sausage” representations highlight the ligand configuration rather than the stereochemistry of the metal complex.

coordination vectors (bite angles ≈ 61 and 63°). An even stronger change in their bite angles is achieved upon light-induced *Z*→*E* isomerization (≈ 137 and 110°).

First, we investigated the photophysical properties of the diazocine ligands and their coordination behaviour independently (Figure 2). Since the formation of multiple species could be expected in the case of incomplete photoswitching,^[14b] Co^{II} was chosen as the metal ion to reduce signal overlap by exploiting the large paramagnetic shifts in the ^1H NMR spectra.^[21] The two ligands were prepared by analogous synthetic strategies (Scheme S1) from either literature-known *p*-diiododiazocine^[22] in two steps (ligand **1**) or 2-nitro-4-iodotoluene in 5 steps (ligand **2**).

The photoswitching properties of ligands **1** and **2** were investigated by NMR (Figures S41, S42, S45, and S46) and UV/Vis spectroscopy (Figures S43, S44, S47 and S48). The ligands were converted from their thermodynamically stable *Z* configuration into the corresponding *E* form by irradiation with light of 385 nm. The photostationary state (PSS) was determined to be 76 % (*E* isomer) for ligand **1** and 72 % for ligand **2** (Figures S42, S46). The thermal half-life ($t_{1/2}$) is 2.0 h for ligand **1** and 5.5 h for ligand **2** at 25°C (Figures S44, S48).

The self-assembly of the ligands (**1-Z**, **1-E**, **2-Z**, **2-E**) with $\text{Co}(\text{BF}_4)_2$ (2:3 metal/ligand ratio) was carried out at room temperature, in particular to prevent relaxation of any metastable self-assemblies composed of **1-E** and **2-E** (Supporting Information Section 3). Complex formation occurs within minutes at room temperature and upon heating the solutions including ligands in their thermodynamically stable *Z* configurations (**1-Z** and **2-Z**) to 50°C , no change of the NMR spectra was observed (Figures S30, S40). Discrete self-assemblies were isolated by precipitation with diethyl ether.

The self-assembly of ligand **1-Z** with $\text{Co}(\text{BF}_4)_2$ exhibits 10 NMR signals within a chemical shift range of approximately 85 ppm (Figure 3a). All signals could be assigned using a combination of paramagnetic NMR methods (Figure 3a).^[21] The fact that the complex exhibits the same number of signals as the free ligand hints at the formation of a highly symmetrical species. The ion peaks and isotope pattern in the ESI mass spectrum (Figure S29) are consistent with the 2:3 Co^{II} /ligand complex $\text{Co}_2(\mathbf{1-Z})_3$. According to NMR experiments, the complex is stable upon dilution to the concentrations required for ESI and UV/Vis measurements (Figure S51).

Photoswitching of $\text{Co}_2(\mathbf{1-Z})_3$ was investigated by irradiation with 385 nm (Figure S52). During irradiation, the ^1H NMR signals assigned to $\text{Co}_2(\mathbf{1-Z})_3$ decrease in intensity and new broad signals are observed (Figure 3a). Only very small signals of the original $\text{Co}_2(\mathbf{1-Z})_3$ remain in the photostationary equilibrium (PSS), which we attribute to the incomplete photoswitching of ligand **1-Z** to **1-E**. The broad signals hint at a mixture of ill-defined species, suggesting the formation of polymers and oligomers. After standing of this solution at room temperature for several hours, the intensities of the ^1H NMR signals for $\text{Co}_2(\mathbf{1-Z})_3$ increase again because **1-E** thermally relaxes back to **1-Z** (Fig-

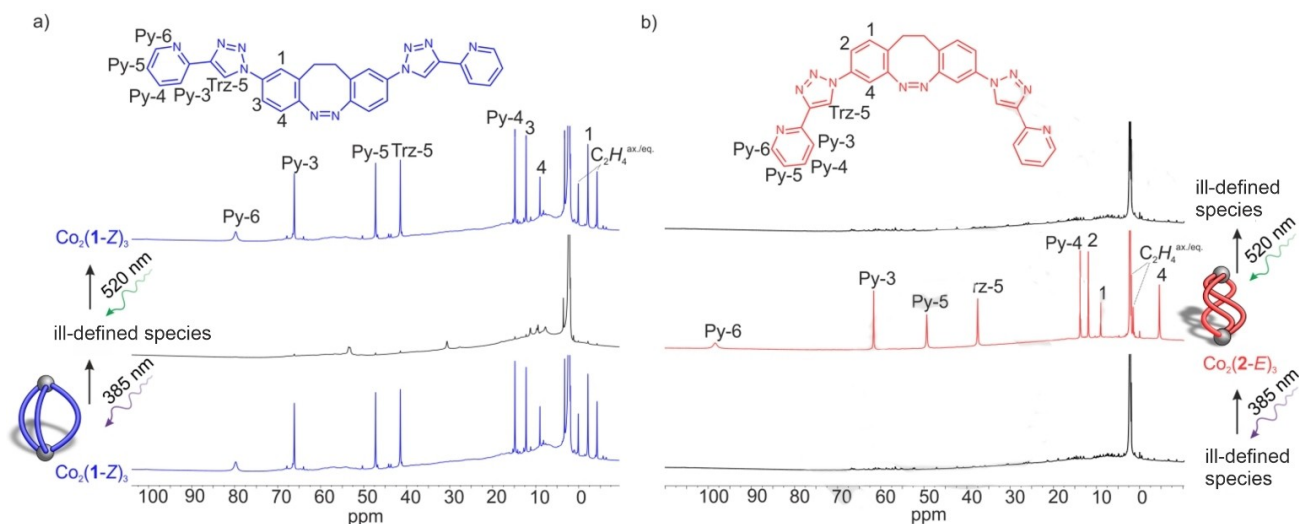


Figure 3. ^1H NMR spectra (CD_3CN , 298 K) of the reversible transformation between: a) $\text{Co}_2(\mathbf{1-Z})_3$ (bottom and top) and the ill-defined species (oligomers) formed with Co^{II} and $\mathbf{1-E}$ (middle) following irradiation with light at 385 nm and 520 nm, respectively; b) the ill-defined mixture formed with Co^{II} and $\mathbf{2-Z}$ (top and bottom) and $\text{Co}_2(\mathbf{2-E})_3$ (middle) following irradiation with light at 385 nm and 520 nm, respectively. Paramagnetic shifts and line broadening are due to the paramagnetic Co^{II} ions.

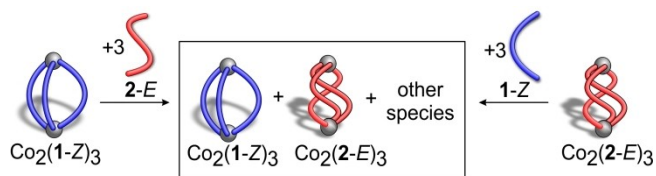


Figure 4. Competition experiments investigating the relative stabilities of $\text{Co}_2(\mathbf{1-Z})_3$ and $\text{Co}_2(\mathbf{2-E})_3$ upon addition of the regioisomeric ligand with the opposite configuration.

ure S50). The thermal half-life ($t_{1/2}$) of ligand $\mathbf{1-E}$ in the presence of Co^{II} ions was measured to be 1.6 h (Figures S52, S53). This half-life is 24 % shorter compared to the free ligand (2.0 h, Figures S43, S44), suggesting the thermal relaxation process is influenced by the metal ions.

Transformation of the ill-defined mixture including ligand $\mathbf{1-E}$ to the discrete helicate $\text{Co}_2(\mathbf{1-Z})_3$ was also achieved by irradiation with green light (520 nm). The conversion is complete within the detection limits of NMR spectroscopy. Photoswitching between the ill-defined mixture and $\text{Co}_2(\mathbf{1-Z})_3$ with 385 and 520 nm is reversible without significant fatigue for 20 cycles by UV/Vis (Figure S54) and ^1H NMR (Figure S49) spectroscopy.

Ligand $\mathbf{2}$ behaves exactly the opposite of ligand $\mathbf{1}$ in the presence of Co^{II} ions. While ligand $\mathbf{1-Z}$ formed the helicate $\text{Co}_2(\mathbf{1-Z})_3$, $\mathbf{2-Z}$ yields a ill-defined mixture (oligomers) (Figure 2b); in contrast to oligomer formation with $\mathbf{1-E}$, the regioisomer $\mathbf{2-E}$ forms the helicate $\text{Co}_2(\mathbf{2-E})_3$ (Figure 3 and Figure S38). $\text{Co}_2(\mathbf{2-E})_3$ is stable to isolation by precipitation (Supporting Information Section 3.2) and dilution (Figure S57). $\text{Co}_2(\mathbf{2-E})_3$ is metastable in solution. The ill-defined mixture is restored due to thermal relaxation of the ligand $\mathbf{2-E}$ back to $\mathbf{2-Z}$ (Figure S56). The half-life was determined to be 9.2 h (Figures S58, S59). This is 67 % longer than the

half-life for the free ligand (5.5 h, Figures S47, S48). The formation of ill-defined species shortens the half-life of $\mathbf{1-E}$ and the formation of a defined triple helicate increases the half-life of ligand $\mathbf{2-E}$.

As in case of the ligand $\mathbf{1}/\text{Co}^{\text{II}}$ system, photoswitching between an ill-defined mixture and a discrete helicate was observed, however, in the reverse direction. Irradiation of ligand $\mathbf{2}$ in the presence of Co^{II} ions (3:2 ratio) with 385 nm yields the discrete helicate $\text{Co}_2(\mathbf{2-E})_3$ and with 520 nm light an ill-defined mixture is formed (Figure 3b). No fatigue was observed over 20 cycles by UV/Vis (Figure S60) and ^1H NMR (Figure S55) spectroscopies.

Hence, ligands $\mathbf{1-Z}$ and $\mathbf{2-E}$ form Co_2L_3 self-assemblies, while ligands $\mathbf{1-E}$ and $\mathbf{2-Z}$ form ill-defined mixtures. Despite numerous attempts, single crystals of $\text{Co}_2(\mathbf{1-Z})_3$ or $\text{Co}_2(\mathbf{2-E})_3$ could not be obtained. To gain more insight into the influence of the structures of the regioisomers and their configurations on the outcome of the self-assembly, theoretical calculations were performed. In principle, complexes $\text{Co}_2(\mathbf{1-Z})_3$ and $\text{Co}_2(\mathbf{2-E})_3$ can exist as helicates or meso-helicates (mesocates). The energies of the four conceivable structures were calculated at the $\omega\text{B97X-D3/def2-TZVP}$ level of theory using ORCA 5.0.1 (Supporting Information Section 7).^[23] In both cases, the helicate was lower in energy (1.2 and 1.8 kcal mol^{-1}) than the mesocate, and thus, we conclude that $\text{Co}_2(\mathbf{1-Z})_3$ and $\text{Co}_2(\mathbf{2-E})_3$ are helicates (Table S4). Helicate structures were also calculated for ligands $\mathbf{1-E}$ and $\mathbf{2-Z}$ and the ligand strain energies in all four helicates were compared (Table S6). Of the ligands in the Z configuration ($\mathbf{1-Z}$ and $\mathbf{2-Z}$), $\text{Co}_2(\mathbf{1-Z})_3$ has a lower ligand strain energy than $\text{Co}_2(\mathbf{2-Z})_3$, and with the ligands in the E configuration, the ligand strain energy for $\text{Co}_2(\mathbf{2-E})_3$ is lower than $\text{Co}_2(\mathbf{1-E})_3$. Ligand $\mathbf{1}$ is more susceptible to form a helicate in its Z configuration and ligand $\mathbf{2}$ prefers to form the helicate in its E configuration. This is in agreement with

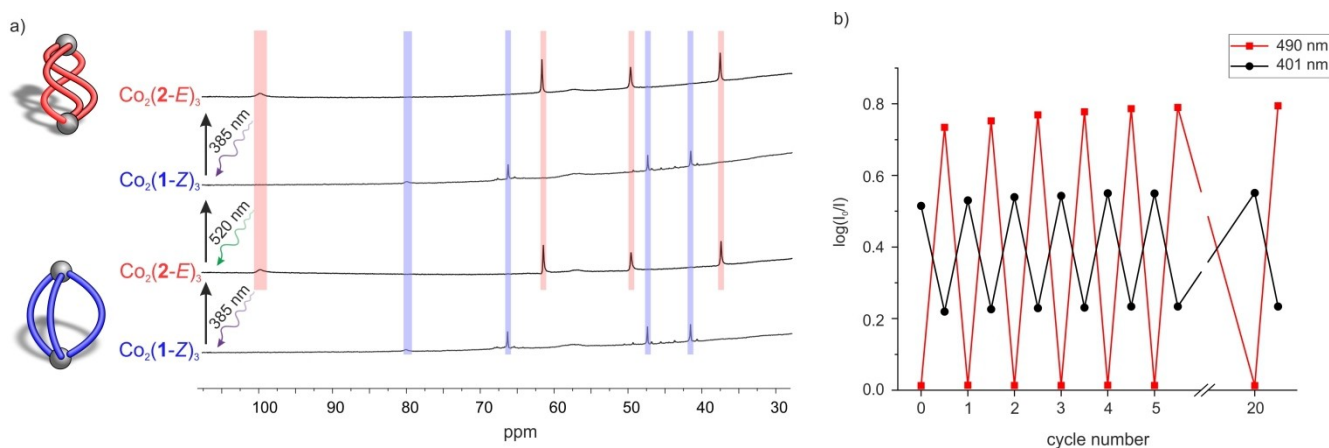


Figure 5. Reversible light-controlled assembly and disassembly of Co₂(1-Z)₃ and Co₂(2-E)₃. A solution of Co₂(1-Z)₃ (a: 6 mM, b: 0.33 mM) was mixed with 3 equivalents of 2-Z and the solution was irradiated with light at 385 and 520 nm in an alternating sequence. a) Bottom spectrum: mainly signals of Co₂(1-Z)₃ are observed (blue shaded). Second spectrum from the bottom: upon irradiation at 385 nm, the signals of Co₂(1-Z)₃ disappear and the signals of Co₂(2-E)₃ appear (red shaded). Third spectrum from the bottom: irradiation at 520 nm restores the signals of Co₂(1-Z)₃ (blue shaded). Note: chemical shift regions below 30 ppm are omitted for clarity. Figure S65 shows the full spectra. Line broadening and the paramagnetic shifts of the ¹H NMR signals are due to ligand coordination to paramagnetic Co^{II} ions. b) Switching stability experiment. The absorption at 401 nm (black) and 490 nm (red) is plotted after alternating irradiation at 385 and 520 nm. Switching is reversible without significant fatigue over 20 cycles.

the experimental findings because Co₂(2-Z)₃ and Co₂(1-E)₃ were experimentally not observed (Figure 4).

Our calculations also predict that the two experimentally observed helicates Co₂(1-Z)₃ and Co₂(2-E)₃ are close in energy. This was corroborated by two complementary experiments by adding: i) ligand 2-E to Co₂(1-Z)₃ (Figures S61, S62); ii) ligand 1-Z to Co₂(2-E)₃ (Figure S63, S64). In both experiments, ligand addition resulted in the formation of a mixture of both Co₂(1-Z)₃ and Co₂(2-E)₃ (Figure 4).

Having demonstrated that discrete self-assemblies are obtained with regioisomeric ligands of the opposite configuration, we envisaged a system where light could be exploited to switch between Co₂(1-Z)₃ and Co₂(2-E)₃, i.e. between helicates of different compositions (Figure 1). In the initial mixture with 1-Z and 2-Z, Co₂(1-Z)₃ forms as the major self-assembled species, as observed by ¹H NMR spectroscopy (Figures 5a and S65). Upon irradiation with 385 nm the signals of Co₂(1-Z)₃ disappear and the signals of Co₂(2-E)₃ grow in. Irradiation with 520 nm induces disassembly of Co₂(2-E)₃ and restores the assembly of Co₂(1-Z)₃ (Figures 5a and S65). Alternating irradiation with 385 nm and 520 nm demonstrated that the transformation between the two helicates is reversible over at least 20 cycles without significant fatigue (Figure 5b).

In conclusion, we report on a self-assembly system including two photoswitchable, diazocine-based ligands (1 and 2) and Co^{II} ions. Both ligands switch to the *E* configuration upon irradiation with violet light (385 nm) and back to the *Z* isomer with green light (520 nm). Among the four possible species 1-Z, 1-E, 2-Z and 2-E, only 1-Z and 2-E form discrete cage-type complexes (helicates) with Co^{II} ions: Co₂(1-Z)₃ and Co₂(2-E)₃. Upon irradiation with 385 nm, Co₂(1-Z)₃ disintegrates and Co₂(2-E)₃ assembles. Irradiation with 520 nm disassembles Co₂(2-E)₃ and Co₂(1-Z)₃ is simultaneously rebuilt. Switching between the two

helicates of different composition exhibits no fatigue or side-products over at least 20 switching cycles (Figure 1 and Figure 5b). Reorganization of multicomponent protein complexes triggered by external stimuli is an ubiquitous phenomenon in signal transduction pathways in nature. Our system might serve as a simple non-biological example and pave the way to the development of more sophisticated systems for artificial signal transduction cascades.

Acknowledgements

We thank the Deutsche Forschungsgemeinschaft (DFG, project number 413396832) for financial support. We thank Friedrich Jurk for synthetic support and NMR data collection for ligand precursors and Dr. Daniel Langbehn for preliminary work. We also thank the spectroscopy department for NMR and mass spectral data collection as well as Dr. Claus Bier and Johanna Baum for performing high-resolution ESI mass spectrometric measurements. Open Access funding enabled and organized by Projekt DEAL.

Conflict of Interest

The authors declare no conflict of interest.

Data Availability Statement

The data that support the findings of this study are available in the Supporting Information of this article.

Keywords: Diazocine · Isomerization · Photochemistry · Self-Assembly · Supramolecular Chemistry

- [1] B. Jastrzebska, P. Ringler, K. Palczewski, A. Engel, *J. Struct. Biol.* **2013**, *182*, 164–172.
- [2] S. J. Wezenberg, *Chem. Lett.* **2020**, *49*, 609–615.
- [3] a) R. Klajn, K. J. M. Bishop, B. A. Grzybowski, *Proc. Natl. Acad. Sci. USA* **2007**, *104*, 10305–10309; b) D. Manna, T. Udayabhaskararao, H. Zhao, R. Klajn, *Angew. Chem. Int. Ed.* **2015**, *54*, 12394–12397; *Angew. Chem.* **2015**, *127*, 12571–12574.
- [4] a) F. Xu, L. Pfeifer, S. Crespi, F. K.-C. Leung, M. C. A. Stuart, S. J. Wezenberg, B. L. Feringa, *J. Am. Chem. Soc.* **2021**, *143*, 5990–5997; b) M. Chen, M. Zhong, J. A. Johnson, *Chem. Rev.* **2016**, *116*, 10167–10211; c) F. D. Jochum, P. Theato, *Chem. Soc. Rev.* **2013**, *42*, 7468–7483.
- [5] F. A. Larik, L. L. Fillbrook, S. S. Nurtila, A. D. Martin, R. P. Kuchel, K. Al Taief, M. Bhadbhade, J. E. Beves, P. Thordarson, *Angew. Chem. Int. Ed.* **2021**, *60*, 6764–6770; *Angew. Chem.* **2021**, *133*, 6838–6844.
- [6] a) A. Ryabchun, Q. Li, F. Lancia, I. Aprahamian, N. Katsonis, *J. Am. Chem. Soc.* **2019**, *141*, 1196–1200; b) T. Fukushima, K. Tamaki, A. Isobe, T. Hirose, N. Shimizu, H. Takagi, R. Haruki, S.-i. Adachi, M. J. Hollamby, S. Yagai, *J. Am. Chem. Soc.* **2021**, *143*, 5845–5854; c) A. Lendlein, H. Jiang, O. Jünger, R. Langer, *Nature* **2005**, *434*, 879–882.
- [7] a) P. Štacko, J. C. M. Kistemaker, T. van Leeuwen, M.-C. Chang, E. Otten, B. L. Feringa, *Science* **2017**, *356*, 964–968; b) N. Koumura, R. W. J. Zijlstra, R. A. van Delden, N. Harada, B. L. Feringa, *Nature* **1999**, *401*, 152–155.
- [8] D. A. Leigh, V. Marcos, T. Nalbantoglu, I. J. Vitorica-Yrezabal, F. T. Yasar, X. Zhu, *J. Am. Chem. Soc.* **2017**, *139*, 7104–7109.
- [9] a) A. J. McConnell, C. S. Wood, P. P. Neelakandan, J. R. Nitschke, *Chem. Rev.* **2015**, *115*, 7729–7793; b) E. Benchimol, B.-N. T. Nguyen, T. K. Ronson, J. R. Nitschke, *Chem. Soc. Rev.* **2022**, *51*, 5101–5135; c) M. J. Burke, G. S. Nichol, P. J. Lusby, *J. Am. Chem. Soc.* **2016**, *138*, 9308–9315; d) T. Y. Kim, R. A. S. Vasdev, D. Preston, J. D. Crowley, *Chem. Eur. J.* **2018**, *24*, 14878–14890.
- [10] a) G. H. Clever, S. Tashiro, M. Shionoya, *J. Am. Chem. Soc.* **2010**, *132*, 9973–9975; b) L. Pesce, C. Perego, A. B. Grommet, R. Klajn, G. M. Pavan, *J. Am. Chem. Soc.* **2020**, *142*, 9792–9802; c) H. Sunohara, K. Koyamada, H. Takezawa, M. Fujita, *Chem. Commun.* **2021**, *57*, 9300–9302.
- [11] N. Kishi, M. Akita, M. Kamiya, S. Hayashi, H.-F. Hsu, M. Yoshizawa, *J. Am. Chem. Soc.* **2013**, *135*, 12976–12979.
- [12] A. J. McConnell, C. J. E. Haynes, A. B. Grommet, C. M. Aitchison, J. Guilleme, S. Mikutis, J. R. Nitschke, *J. Am. Chem. Soc.* **2018**, *140*, 16952–16956.
- [13] S. M. Jansze, G. Cecot, K. Severin, *Chem. Sci.* **2018**, *9*, 4253–4257.
- [14] a) E. Britton, R. J. Ansell, M. J. Howard, M. J. Hardie, *Inorg. Chem.* **2021**, *60*, 12912–12923; b) A. D. W. Kennedy, R. G. DiNardi, L. L. Fillbrook, W. A. Donald, J. E. Beves, *Chem. Eur. J.* **2022**, *28*, e202104461; c) R. DiNardi, A. O. Douglas, R. Tian, J. Price, M. Tajik, W. A. Donald, J. Beves, *Angew. Chem. Int. Ed.* **2022**, *61*, e202205701; *Angew. Chem.* **2022**, *134*, e202205701.
- [15] a) M. Han, R. Michel, B. He, Y.-S. Chen, D. Stalke, M. John, G. H. Clever, *Angew. Chem. Int. Ed.* **2013**, *52*, 1319–1323; *Angew. Chem.* **2013**, *125*, 1358–1362; b) M. Han, Y. Luo, B. Damaschke, L. Gómez, X. Ribas, A. Jose, P. Peretzki, M. Seibt, G. H. Clever, *Angew. Chem. Int. Ed.* **2016**, *55*, 445–449; *Angew. Chem.* **2016**, *128*, 456–460; c) R.-J. Li, J. J. Holstein, W. G. Hiller, J. Andréasson, G. H. Clever, *J. Am. Chem. Soc.* **2019**, *141*, 2097–2103.
- [16] C. Stuckhardt, D. Roke, W. Danowski, E. Otten, S. J. Wezenberg, B. L. Feringa, *Beilstein J. Org. Chem.* **2019**, *15*, 2767–2773.
- [17] H. Lee, J. Tessarolo, D. Langbehn, A. Baksi, R. Herges, G. H. Clever, *J. Am. Chem. Soc.* **2022**, *144*, 3099–3105.
- [18] a) J. B. Trads, K. Hüll, B. S. Matsuura, L. Laprell, T. Fehrentz, N. Görlt, K. A. Kozek, C. D. Weaver, N. Klöcker, D. M. Barber, D. Trauner, *Angew. Chem. Int. Ed.* **2019**, *58*, 15421–15428; *Angew. Chem.* **2019**, *131*, 15567–15574; b) M. Schehr, C. Ianes, J. Weisner, L. Heintze, M. P. Müller, C. Pichlo, J. Charl, E. Brunstein, J. Ewert, M. Lehr, U. Baumann, D. Rauh, U. Knippschild, C. Peifer, R. Herges, *Photochem. Photobiol. Sci.* **2019**, *18*, 1398–1407.
- [19] T. Tellkamp, J. Shen, Y. Okamoto, R. Herges, *Eur. J. Org. Chem.* **2014**, 5456–5461.
- [20] M. H. Burk, D. Langbehn, G. Hernández Rodríguez, W. Reichstein, J. Drewes, S. Schröder, S. Rehders, T. Strunskus, R. Herges, F. Faupel, *ACS Appl. Polym. Mater.* **2021**, *3*, 1445–1456.
- [21] M. Lehr, T. Paschelke, E. Trumpf, A.-M. Vogt, C. Näther, F. D. Sönnichsen, A. J. McConnell, *Angew. Chem. Int. Ed.* **2020**, *59*, 19344–19351; *Angew. Chem.* **2020**, *132*, 19508–19516.
- [22] M. S. Maier, K. Hüll, M. Reynders, B. S. Matsuura, P. Leippe, T. Ko, L. Schäffer, D. Trauner, *J. Am. Chem. Soc.* **2019**, *141*, 17295–17304.
- [23] a) F. Weigend, R. Ahlrichs, *Phys. Chem. Chem. Phys.* **2005**, *7*, 3297–3305; b) F. Weigend, *Phys. Chem. Chem. Phys.* **2006**, *8*, 1057–1065; c) F. Neese, F. Wennmohs, A. Hansen, U. Becker, *Chem. Phys.* **2009**, *356*, 98–109; d) S. Grimme, J. Antony, S. Ehrlich, H. Krieg, *J. Chem. Phys.* **2010**, *132*, 154104; e) Y.-S. Lin, G.-D. Li, S.-P. Mao, J.-D. Chai, *J. Chem. Theory Comput.* **2013**, *9*, 263–272; f) M. Miklitz, K. E. Jelfs, *J. Chem. Inf. Model.* **2018**, *58*, 2387–2391; g) C. Bannwarth, S. Ehlert, S. Grimme, *J. Chem. Theory Comput.* **2019**, *15*, 1652–1671; h) F. Neese, F. Wennmohs, U. Becker, C. Riplinger, *J. Chem. Phys.* **2020**, *152*, 224108; i) C. Bannwarth, E. Caldeweyher, S. Ehlert, A. Hansen, P. Pracht, J. Seibert, S. Spicher, S. Grimme, *WIREs Comput. Mol. Sci.* **2021**, *11*, e1493.

Manuscript received: August 26, 2022

Accepted manuscript online: October 10, 2022

Version of record online: November 29, 2022